Advances in Materials Research, *Vol. 11, No. 3 (2022) 225-235*
https://doi.org/10.12989/amr.2022.11.3.225

Synthesis, characterization and potential applications of Ag@ZnO nanocomposites with S@g-C_3N_4

Naveed Ahmad [1,2], Mohsin Javed [1], Muhammad A. Qamar*[1], Umbreen Kiran [1], Sammia Shahid [1], Muhammad B. Akbar [3], Mudassar Sher [1] and Adnan Amjad [1]

[1] *Department of Chemistry, University of Management and Technology, Lahore, Pakistan*
[2] *Department of Chemistry, University of Turin Via Pietro Giuria 5, 10125 Turin, Italy*
[3] *National Center for Nanoscience Technology (NCNST), No. 11, Zhong Guan Cun Bei Yitiao, 100190 Beijing, P.R. China*

(*Received September 16, 2019, Revised August 30, 2021, Accepted March 23, 2022*)

Abstract. It includes the synthesis of pristine ZnO nanoparticles and a series of Ag-doped zinc oxide nanoparticles was carried out by reflux method by varying the amount of silver (1, 3, 5, 7 and 9% by mol.). The morphology of these nanoparticles was investigated by SEM, XRD and FT-IR techniques. These techniques show that synthesized particles are homogenous spherical nanoparticles having an average particle size of about 50-100 nm along with some agglomeration. The photocatalytic activity of the ZnO nanoparticles and Ag doped ZnO nanoparticles were investigated via photodegradation of methylene blue (MB) as a standard dye. The data from the photocatalytic activity of these nanoparticles show that 7% Ag-doped ZnO nanoparticles exhibit much enhanced photocatalytic activity as compared to pristine ZnO nanoparticles and other percentages of Ag-doped ZnO nanoparticles. Furthermore, 7% Ag-doped ZnO was made composites with sulfur-doped graphitic carbon nitride by physical mixing method and a series of nanocomposites were made (3.5, 7.5, 25, 50, 75% by weight). It was observed that the 25% composites exhibited better photocatalytic performance than pristine S-g-C 3 N 4 and pure 7% Ag-doped ZnO. Tauc's plot also supports the photodegradation results.

Keywords: composites; nanoparticles; photocatalytic activity; photodegradation; S-g-C_3N_4; ZnO

1. Introduction

Discharge of industrial wastes into the marine systems cause severe water pollution which is one of the major environmental concerns craving immediate attention. Toxic and colored organic pollutants are the crucial factors polluting natural water sources up to dangerous limits. Photocatalytic degradation of organic pollutants is one of the simplistic, low- cost, green and environmentally friendly technologies being utilized (Hussain *et al*. 2017, Iqbal *et al*. 2017). Semiconductor materials such as SnO_2, CuO, TiO_2 and ZnO and have been recognized as efficient photocatalysts (Pare *et al*. 2008, Kim *et al*. 2016). ZnO is of special interest because of its suitable direct bandgap (~3.2 eV), exciton binding energy (60 meV), high redox potential and high electron mobility. However, its fast recombination of electron-hole pairs, photocorrosion, and limited

*Corresponding author, E-mail: qamariub@gmail.com

http://www.techno-press.org/?journal=amr&subpage=5 ISSN: 2234-0912 (Print), 2234-179X (Online)

visible light absorbance confine its widespread application. Extensive research have been therefore focused on overcoming these drawbacks, by surface sensitization with dyes and metal complexes, by hybridizing with other semiconductors and doping/co-doping with metal, non-metal and noble metal ions (Kumar and Rao 2015). Among these techniques, merging ZnO with other semiconductors and doping with metals to form a heterojunction with a suitable band structure can efficiently improve light-absorption range as well as the frequency of electron-hole pair separation. It is recognized well that metal doping of ZnO leads to a decrease in band gap and tends to modify it into a visible-light-active photocatalyst (Thi and Lee 2017). Metal doping of ZnO allows it to absorb visible radiations of the solar spectrum by producing deep-level states without changing the bandgap. Studies revealed that ZnO doping with Ag leads to a red-shift and increases its photocatalytic efficiency in the visible-light region. Ag metal is a good conductor, can act as a sink for free electrons, and increases the separation rates of photoinduced electron-hole pairs (Jing *et al*. 2016, Jaramillo-Páez *et al*. 2017). In photocatalytic applications, carbon materials such as graphitic carbon nitride (g-C_3N_4) has been recognized as the most stable allotrope of carbon nitride due to its exceptional thermal, optical, mechanical, electrical properties and eco-friendly nature (Zhang *et al*. 2015, Wang *et al*. 2009). It has a bandgap of about 2.7 eV and can absorb visible light up to 450 nm (Kuriki *et al*. 2015, Chen *et al*. 2015). However, the photocatalytic efficiency of pristine g-C_3N_4 is restricted due to its low surface area (< 10 m^2/g), inadequate visible light absorption capacity, and particularly fast recombination of photogenerated electron-hole pairs (Zhang *et al*. 2016). In order to mend its photocatalytic efficiency, many approaches have been applied. Due to its polymeric nature, its surface chemistry can be modified by surface engineering without obviously altering the theoretical composition (Ali and Gupta 2016, Iqbal *et al*. 2020). The photocatalytic activity of pristine g-C_3N_4 has been improved by applying different modification approaches such as nanoarchitecture design by hard/soft templating, elemental doping, molecular doping, exfoliation and synthesis of g-C_3N_4/metal oxides heterojunctions (Wang *et al*. 2011, Dong *et al*. 2012). Particularly, when g-C_3N_4 is doped with sulfur its band gap is narrows and visible-light absorption is enhanced. The doped sulphur stacks its 2p orbitals on the valence band of pristine g-C_3N_4 and modifies its band structure (Liu *et al*. 2010). Among stated approaches, anion doping plays a prime role to modify the physicochemical properties of g-C_3N_4. In this method dopants are introduced homogeneously as impurities into the host backbone which lead to the creation of localized states in bandgap (Liu *et al*. 2010, Jourshabani *et al*. 2017). This phenomenon not only increases visible light absorption but also enhance the mobility photogenerated charge carries (Sher *et al*. 2021a, Ran *et al*. 2015). S-doping improves the charge carrier mobility and accelerates the separation of photogenerated electron-hole pairs in S-g-C_3N_4 (Feng *et al*. 2014). For example, Hong *et al*. stated that sulfur-doped mesonanoporous g-C_3N_4 synthesized by hard templating method showed 30 times more photocatalytic H2-production activity than pristine g-C_3N_4 (Hong *et al*. 2012). Similarly, sulfur-doped g-C_3N_4 synthesized by heating thiourea and melamine mixtures showed solar radiation absorption extension to near IR region (up to 475 nm), and its photocatalytic CO_2 reduction rate was 1.38 times higher than un-doped g-C_3N_4 (Wang *et al*. 2015, Qamar *et al*. 2021a). Both theoretically and experimentally, it has been proven that doping of sulphur and nitrogen substitution revised the structure of g-C_3N_4, lessened the bandgap energy and tuned the conduction and valence band levels. S doped g-C_3N_4 exhibited better carrier mobility and efficient electron-hole pair separation efficiency (Jiang *et al*. 2017, Irfan *et al*. 2019). To make the stable and proficient photocatalyst, combining the property of both sulfur-doped g-C_3N_4 and Ag-ZnO to extend the spectral response looks exceptionally vital. In the present article, ZnO and Ag-doped ZnO (1, 3, 5, 7, and 9%) nanoparticles were synthesized by the Reflux method.

Afterward, the photocatalytic activity of these samples was analyzed by the photo-degradation of methylene blue (MB) dye under sunlight irradiation. Among the samples mentioned above, 7% Ag-doped ZnO nanoparticles showed optimum photocatalytic degradation of MB. Then, the 7% Ag-doped ZnO nanoparticles having optimum results were made composite with sulfur-doped graphitic carbon nitride to obtain a series of novel nanocomposites (3.5, 7.5, 25, 50, and 75%) by combining respective quantities of 7% Ag-doped ZnO nanoparticles with sulfur-doped graphitic carbon nitride. The synthesized samples were characterized by scanning electron microscope (SEM), X-ray diffraction (XRD) and Fourier transforms infrared spectroscopy (FTIR) and Tauc's Plot study. A UV-Vis spectrophotometer was used to carry out the degradation study of methylene blue by synthesized samples.

2. Experimental details

Following reagents and chemicals are required for the synthesis of ZnO, Ag doped ZnO and for S-doped g-C_3N_4.

2.1 Chemicals

Zinc Nitrate Hexa-hydrate ($Zn(NO_3)2.6H_2O$), Silver Nitrate ($AgNO_3$), Sodium Hydroxide (NaOH), Thiourea ($(NH_2)2CS$), De-ionized water and Ethanol (C_2H_5OH). All reagents and chemicals were obtained from Sigma-Aldrich and used as received without further purification.

2.2 Synthesis of Pure ZnO Nanoparticles

For the synthesis of ZnO nanoparticles, 0.05M (14.8735 g) of $Zn(NO3)2.6H_2O$ were dissolved in 100 ml of de-ionized water. The solution was kept on stirring at room temperature for 30 minutes. 2M NaOH was added slowly to maintain the pH to 11. In order to obtain NPs, the final solution was transferred to round bottom flask for heating and refluxing at optimized conditions i.e., for 6 h at 60 ± 1°C. After reaction completion, the solution was cooled to room temperature and white precipitates were collected. This was further washed several times with D.I. water and ethanol. The powder was then further dried at 70°C for 3 hours.

2.3 Synthesis of Ag doped ZnO Nanoparticles

1% Ag-doped ZnO NPs was prepared by following a similar method as described above. 1% molar equivalent amount of $AgNO_3$ was added to 25 ml solution of $Zn(NO_3)_2.6H_2O$ (0.05 M) followed by the addition of 25 ml solution of NaOH (2M) dropwise and continue stirring till precipitate form due to formation of respective hydroxides. Then the solution was transferred to round bottom flask for heating and refluxing at optimized conditions i.e., for 6 h at 60 ± 1°C. After the reaction completion, grayish-white precipitates were obtained. The precipitates were washed with D.I. and ethanol several times to remove the unwanted salts. The powder further dried in an oven at 70°C for 3 h. The same procedure was adopted for the synthesis of 3, 5, 7, and 9% Ag-ZnO NPs (Kumar *et al*. 2015).

2.4 Synthesis of sulfur-doped g-C_3N_4 (S- g-C_3N_4)

In a typical procedure to synthesize S-g-C_3N_4, 30 g of Thiourea (NH)2CS was placed in separate three ceramic crucibles covered with lid in a Muffle furnace at 520°C for 2 hours at the

rate of 5°C/mint. Subsequently, after naturally cooling at room temperature, a yellowish product was obtained, which was ground, and collected in samples vials. Further, the product was used for photocatalytic activity and for making composites (Wang *et al*. 2015).

2.5 Synthesis of composites

To prepare nanocomposites, a specific quantity of 7% Ag-ZnO NPs was dispersed in 100 ml deionized water, sonicated for 15 minutes, and stirred for the next 1hour. In a separate beaker, the fixed quantity of S-g-C_3N_4 was dispersed in 100 ml D.I water, sonicated for 15 minutes, and stirred for the next 1 hour. Then, these solutions were added dropwise into a separate beaker fixed in an ice bath and continue stirring for 1.5 hours. The subsequent nanocomposites were filtered, dried, and saved. A series of composites (3.5, 7.5, 25, 50 & 75%) was prepared by repeating this procedure.

3. Photocatalytic activity

The photocatalytic activity of the prepared nanoparticles and nanocomposites was judged by the photocatalytic degradation of Methylene blue (MB), an organic dye. A 0.05 g catalyst was added to 100 ml of MB solution. The solutions of the samples and dye were prepared in tap water (pH = 6-7). First of all, the photocatalyst was placed in an aqueous solution of MB under dark for half-hour to attain adsorption-desorption equilibrium. The UV-Vis spectrum of the sample was taken via UV-Vis spectrophotometer (JASCO 770) after centrifugation to separate the residual catalyst. Further, the solution of dye-containing nanosample was placed in sunlight in an open atmosphere in a 250 ml petri dish. After regular intervals, 6ml of the dye solution was taken out and scanned by UV-Vis spectrum.

4. Results and discussion

The surface morphology of as-synthesized samples was characterized by scanning electron microscopy (TESCAN Vega 3). Fig. 1(a) shows the SEM image of pure ZnO nanoparticles. The average diameter of the particles is about 40-100 nm, along with some agglomeration. Fig. 1(b)

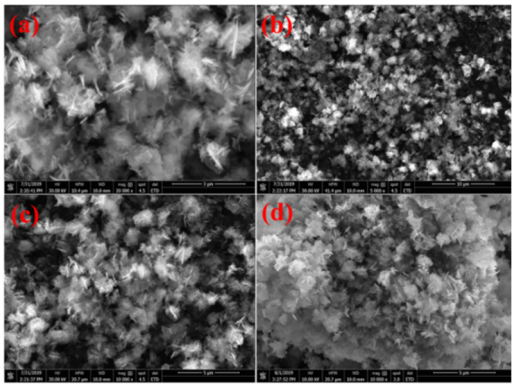

Fig. 1 SEM Images (a) Pure ZnO; (b) Ag-ZnO; (c) S-g-C_3N_4; (d) 7% Ag-ZnO /25% S-g-C_3N_4

shows the SEM image of 7% Ag-ZnO NPs. These NPs are of size 80-100 nm and exhibit some

degree of coagulation. Fig. 1(c) shows the SEM image of S-g-C_3N_4 layers and these nano-size layers are exhibit some coalescence. Fig. 1(d) shows the 7% Ag-ZnO/25% S-g-C_3N_4 composite in which the Ag-ZnO NPs are uniformly distributed over the sulphur doped graphitic carbon nitride along with some aggregation.

The crystallinity of the samples was investigated by X-ray diffraction spectrometer (PAN analytical X' Pert). Fig. 2 shows the XRD patterns of as-synthesized nanoparticles as well as composites. All the prominent characteristic peaks of ZnO are shown here by the symbol "*" exhibiting the hexagonal wurtzite structure in the XRD pattern of ZnO, while the Ag-ZnO NPs shows the ZnO as well as Ag peaks. The Ag peaks are indicated by the symbol "#" exhibiting the face-centered cubic (fcc) structure as reported by the literature also (Height *et al*. 2006). No other impurities are observed. The XRD pattern of sulfur-doped graphitic carbon nitride showing the prominent peak (002) at 2θ° = 27, which is the characteristic peak of S-g-C_3N_4 (Wang *et al*. 2015). The XRD patterns of composites showing all the reference peaks of ZnO, Ag and S-g-C_3N_4. Hence it is confirmation of the formation of composites. The average crystallite size of ZnO NPs calculated by Scherrer's equation was found to be 24.11 nm.

Fig. 3 shows the FT-IR spectrum of synthesized samples between the ranges of 400–4000 cm^{-1}. The peaks that appeared from 500 cm^{-1} to 1000 cm^{-1} are due to the stretching and rocking vibration

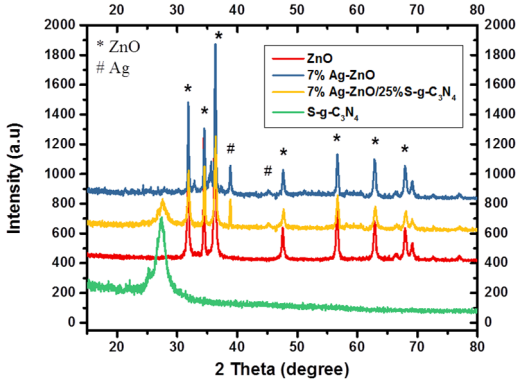

Fig. 2 XRD of ZnO, Ag Doped ZnO, S-g-C_3N_4 and 7% Ag-ZnO/25% S-g-C_3N_4

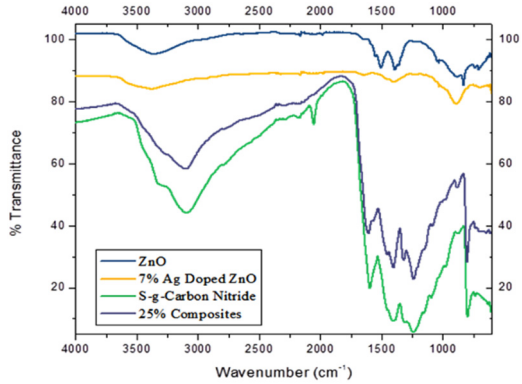

Fig. 3 FTIR spectra of ZnO, Ag-ZnO, S-g-C_3N_4 and 7% Ag-ZnO/25% S-g-C_3N_4

modes in pure ZnO, while the broad peak at 3364.89 cm^{-1} refers to the presence of the OH group

(Alwan *et al*. 2015). The sharp peak at 1506.26 cm^{-1} is responsible for bending vibrations of H-O-H, which indicates the presence of H_2O in ZnO nanoparticles. In the FTIR spectrum of Ag-ZnO, the main peak at 622.05 cm^{-1} is due to Zn-O stretching vibration mode, while the peak at 888.52 cm^{-1} is due to the doped silver. The peaks at 1404.80 cm^{-1} occur due to H-O-H deformation vibrations and at 3374.44 cm^{-1} refers to the presence of the OH group (Khan *et al*. 2013). In the FTIR spectrum of S-g-C_3N_4, the vibrational frequency at 800.22 cm^{-1} is characteristic of triazine in condensed CN heterocycles and some peaks from 1250 cm^{-1} to 1600 cm^{-1} are responsible for stretching vibration modes of heptazine heterocyclic ring (C_6N_7). Nonappearance of any bands assigned to the S-containing group's vibrations can be attributed to a slight amount of the S atoms and to the superposition of C-S vibrational modes with CN vibrations at 1200-1050 cm^{-1}. A weak band is observed at 2150 cm^{-1} is due to the absorption of CO_2 from the atmosphere (Qamar *et al*. 2020a, 2021b, Wang *et al*. 2015). The FTIR spectrum of composite contains all corresponding peaks of the metal-oxygen bond, doped metal, and relative peaks of S-g-C_3N_4, confirming the successful formation of the composite.

Energy band gap of as synthesized materials were determined using Tauc's plot. In Fig. 4 the band gap of ZnO was calculated and determined out to be almost 3 eV. As ZnO was doped with Ag metal then the bandgap of the Ag-ZnO NPs is decreased because doping reduces the band gap by creating some energy levels below the conduction band and its absorption in visible region is enhanced (Qamar *et al*. 2017). So, Ag doping motives an extensive absorbance by Ag-ZnO NPs in the visible region which supports its decreased bandgap.7% Ag doped ZnO showed lowest band gap as 2.32 eV among all other Ag doped ZnO nanoparticles (1, 3, 5, 9 by mmol%). The bandgap of 7% Ag-ZnO/25%S-g-C_3N_4 nanocomposites is further reduced to 2.17 eV.

A series of photodegradation experiments were performed to study the photocatalytic activity of different samples using MB as an ideal pollutant under sunlight. Fig. 5(a) shows the variation in degradation of MB concentration with irradiation time using Ag-ZnO nanoparticles.

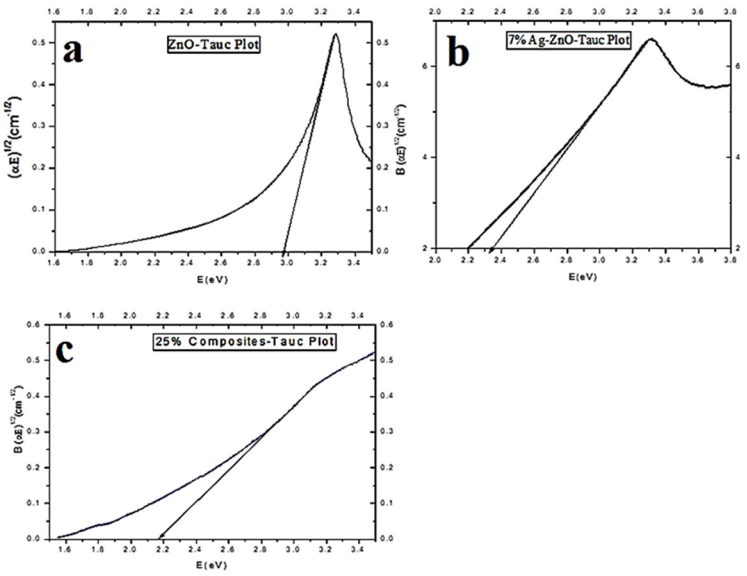

Fig. 4 Tauc's Plot of ZnO, Ag-ZnO, S-g-C_3N_4 and 7% Ag-ZnO/25% S-g-C_3N_4

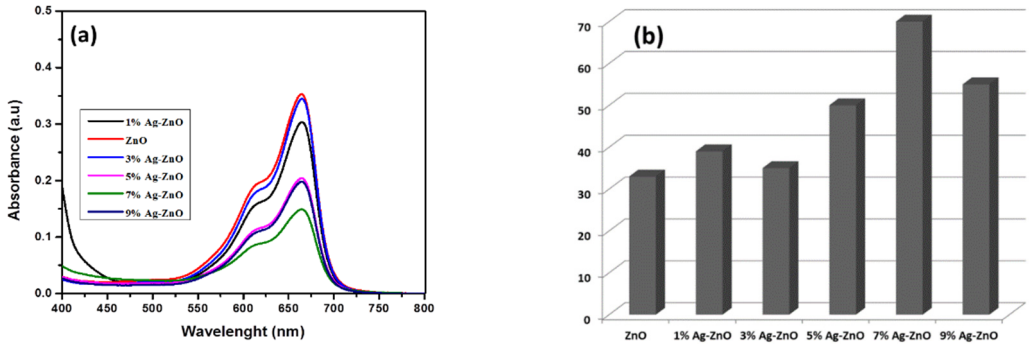

Fig. 5 Comparison of photocatalytic degradation of MB by Ag-ZnO NPs (a) % degradation of dye after 2.5 hour under sunlight (b)

In the first round all the synthesized ZnO and Ag-ZnO NPs were assessed for photodegradation potential. The photocatalytic experiments were performed in a very systematic way. The percentage degradation of the MB dye under sunlight is shown in Fig. 5(b). Ag-ZnO NPs exhibited much batter photocatalytic activity than pristine ZnO because the Ag act as electron sinks, which not only extend the life span of electron and holes but also enhance the separation efficiency of e-h pairs. Thus, the photocatalytic efficiency of the Ag-ZnO NPs is improved under visible light after doping ZnO with Ag. 7% Ag doped ZnO exhibited batter photocatalytic activity (70%) among all other Ag doped ZnO (1, 3, 5, 9 mmol%). The significant improvement in photocatalytic performance of 7% Ag-ZnO NPs is due to improved electron trap sites and its lower bandgap energy than other Ag-ZnO NPs (1, 3, 5, 9 mmol%) (Iqbal *et al*. 2017). The weak photocatalytic activity of ZnO is due to its large bandgap and low absorption in the visible region of solar spectrum. In the second step, 7% Ag-ZnO NPs was integrated to S-g-C_3N_4 nanosheets to produce visible light responsive photocatalysts. Then the relative MB photodegradation rates of 7%Ag-ZnO/S-g-C_3N_4 nanocomposites with variable S-g-C_3N_4 (3.5, 7.5, 25, 50, and 75 wt.%) concentrations were evaluated. The maximum photodegradation rate was found with 25 wt.% S-g-C_3N_4 loading, indicating an effective photodegradation rate (98.13%) under sunlight illumination (After 2.5 hours). Further, it was found that enhancing the S-g-C_3N_4 contents beyond this amount, lead to a decrease of the photodegradation efficiency and the MB photodegradation was reduced to 73% with 75 wt.% S-g-C_3N_4 contents. Ag-ZnO nanoparticles attached on S-g-C_3N_4 sheets acts as electron traps and reduce e-h recombination. These trapped electrons are then transferred to the absorbed O_2 which act as an electron acceptor. The photogenerated electrons reduce O_2 into superoxide anions (O^{-}_{2}), and further holes and superoxide anions produce OH• radicals from chemisorbed H_2O molecules (Qamar *et al*. 2020b, 2021c, Linsebigler *et al*. 1995). These reactive oxygen species then degrade MB dye molecules. So, the efficient charge separation of photogenerated e-h was achieved which is responsible for the enhanced photocatalytic efficiency of the Ag-ZnO/ S-g-C_3N_4 as compared to its counter parts (Subramanian *et al*. 2001, Kuo and Ho 2001). The degradation rate was calculated using the degradation efficiency equation as follows

$$D\% = \frac{C_0 - C}{C_0} \times 100 \quad (1)$$

Where C_0 is initial concentration and C is the concentration after "*t*" minutes of light irradiation.

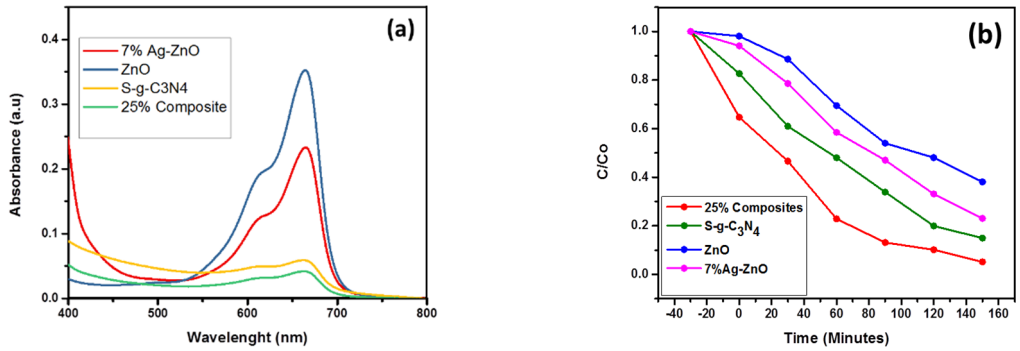

Fig. 6 Comparison of photocatalytic degradation of MB by ZnO, Ag-ZnO, Ag-ZnO/S-g-C_3N_4 and S-g-C_3N_4 in 2.5 hour under sunlight (a) dye degradation rate MB by ZnO, Ag-ZnO, Ag-ZnO /S-g-C_3N_4 and S-g-C_3N_4 samples (b)

The degradation efficiency was calculated including adsorption-desorption and photodegradation. The corresponding % degradation (dye degradation) results of the prepared nanocomposites are presented in Figs. 6(a)-(b). From Figs. 6(a)-(b), it is evident that 25% composite exhibited maximum photocatalytic efficiency and degraded 98.13% MB in 2.5 hours.

5. Conclusions

An efficient Ag-ZnO/ S-g-C_3N_4 visible-light-driven photocatalyst synthesized by integrating Ag-doped ZnO NPs with S-g-C_3N_4 in a single step by hydrothermal route. The co-occurrence of diffraction peaks of ZnO, Ag, and S-g-C_3N_4 in the XRD pattern of Ag-ZnO/S-g-C_3N_4 confirmed the formation of its heterostructure. Ag-doped ZnO NPs are evenly distributed over S-g-C_3N_4 layers. The morphology of the NPs was found to be spherical having size about 50-100 nm. 7% Ag-doped ZnO NPs show best photodegradation results among the Ag doped (1, 3, 5, 7 and 9%) series and degrade 70% MB in 2.5 hours. Among the series of 7%Ag-ZnO NPs integrated with S-g-C_3N_4, the 7%Ag-ZnO/25% S-g-C_3N_4 nanocomposite exhibited outstanding efficiency and degraded 98.13% MB in 2.5 hours. Tauc plot bandgap values also supported the best photocatalytic efficiency of 7%Ag-ZnO/25% S-g-C_3N_4 nanocomposite. Thus, in the future, 7%Ag-ZnO/25% S-g-C_3N_4 nanocomposite likely to be applied for environmental remediation applications.

References

Ali, I. and Gupta, V.K. (2006), "Advances in water treatment by adsorption technology", *Nat. Protoc.*, **1**(6), 2661-2667. https://doi.org/10.1038/nprot.2006.370

Alwan, R.M., Kadhim, Q.A., Sahan, K.M., Ali, R.A., Mahdi, R.J., Kassim, N.A. and Jassim, A.N. (2015), "Synthesis of zinc oxide nanoparticles via sol–gel route and their characterization", *Nanosci. Nanotechnol.*, **5**(1), 1-6. https://doi.10.5923/j.nn.20150501.01

Anwer, S., Anjum, D.H., Luo, S., Abbas, Y., Li, B., Iqbal, S. and Liao, K. (2021), "2D Ti3C2Tx MXene nanosheets coated cellulose fibers based 3D nanostructures for efficient water desalination", *Chem. Eng. J.*, **406**, 126827. https://doi.org/10.1016/j.cej.2020.126827

Chen, S., Wang, C., Bunes, B.R., Li, Y., Wang, C. and Zang, L. (2015), "Enhancement of visible-light-

driven photocatalytic H_2 evolution from water over g-C_3N_4 through combination with perylene diimide aggregates", *Appl. Catal. A: General*, **498**, 63-68. https://doi.org/10.1016/j.apcata.2015.03.026

Dong, G., Zhao, K. and Zhang, L. (2012), "Carbon self-doping induced high electronic conductivity and photoreactivity of g-C_3N_4", *Chem. Commun.*, **48**(49), 6178-6180. https://doi.org/10.1039/C2CC32181E

Feng, L.L., Zou, Y., Li, C., Gao, S., Zhou, L.J., Sun, Q., Fan, M., Wang, H., Wang, D., Li, G.D. and Zou, X. (2014), "Nanoporous sulfur-doped graphitic carbon nitride microrods: a durable catalyst for visible-light-driven H_2 evolution", *Int. J. Hydrogen Energy*, **39**(28), 5373-15379. https://doi.org/10.1016/j.ijhydene.2014.07.160

Height, M.J., Pratsinis, S.E., Mekasuwandumrong, O. and Praserthdam, P. (2006), "Ag-ZnO catalysts for UV-photodegradation of methylene blue", *Appl. Catal. B: Environ.*, **63**(3-4), 305-312. https://doi.org/10.1016/j.apcatb.2005.10.018

Hong, J., Xia, X., Wang, Y. and Xu, R. (2012), "Mesoporous carbon nitride with in situ sulfur doping for enhanced photocatalytic hydrogen evolution from water under visible light", *J. Mater. Chem.*, **22**(30), 15006-15012. https://doi.org/10.1039/C2JM32053C

Hussain, W., Badshah, A., Hussain, R.A., Aleem, M.A., Bahadur, A., Iqbal, S., Farooq, M.U. and Ali, H. (2017), "Photocatalytic applications of Cr_2S_3 synthesized from single and multi-source precursors", *Mater. Chem. Phys.*, **194**, 345-355. https://doi.org/10.1016/j.matchemphys.2017.04.001

Iqbal, S. (2020), "Spatial charge separation and transfer in L-cysteine capped NiCoP/CdS nano-heterojunction activated with intimate covalent bonding for high-quantum-yield photocatalytic hydrogen evolution", *Appl. Catal. B: Environ.*, **274**, 119097. https://doi.org/10.1016/j.apcatb.2020.119097

Iqbal, S., Pan, Z. and Zhou, K. (2017), "Enhanced photocatalytic hydrogen evolution from in situ formation of few-layered MoS_2/CdS nanosheet-based van der Waals heterostructures", *Nanoscale*, **9**(20), 6638-6642. https://doi.org/10.1039/C7NR01705G

Iqbal, S., Javed, M., Bahadur, A., Qamar, M.A., Ahmad, M., Shoaib, M., Raheel, M., Ahmad. N., Akbar. M.B. and Li, H. (2020), "Controlled synthesis of Ag-doped CuO nanoparticles as a core with poly (acrylic acid) microgel shell for efficient removal of methylene blue under visible light", *J. Mater. Sci.: Mater. Electron.*, **31**(11), 8423-8435. https://doi.org/10.1007/s10854-020-03377-9

Irfan, R.M., Tahir, M.H., Khan, S.A., Shaheen, M.A., Ahmed, G. and Iqbal, S. (2019), "Enhanced photocatalytic H_2 production under visible light on composite photocatalyst (CdS/NiSe nanorods) synthesized in aqueous solution", *J. Colloid Interface Sci.*, **557**, 1-9. https://doi.org/10.1016/j.jcis.2019.09.014

Irfan, R.M., Tahir, M.H., Maqsood, M., Lin, Y., Bashir, T., Iqbal, S., Zhao, J., Gao, L. and Haroon, M. (2020), "CoSe as non-noble-metal cocatalyst integrated with heterojunction photosensitizer for inexpensive H_2 production under visible light", *J. Catal.*, **390**, 196-205. https://doi.org/10.1016/j.jcat.2020.07.034

Jaramillo-Páez, C., Navío, J.A., Hidalgo, M.C. and Macías, M. (2017), "High UV- photocatalytic activity of ZnO and Ag/ZnO synthesized by a facile method", *Catal. Today*, **284**, 121-128. https://doi.org/10.1016/j.cattod.2016.11.021

Jiang, L., Yuan, X., Pan, Y., Liang, J., Zeng, G., Wu, Z. and Wang, H. (2017), "Doping of graphitic carbon nitride for photocatalysis: a review", *Appl. Catal. B: Environ.*, **217**, 388-406. https://doi.org/10.1016/j.apcatb.2017.06.003

Jing, L., Xu, Y., Huang, S., Xie, M., He, M., Xu, H., Li, H. and Zhang, Q. (2016), "Novel magnetic $CoFe_2O_4$/Ag/Ag_3VO_4 composites: Highly efficient visible light photocatalytic and antibacterial activity", *Appl. Catal. B: Environ.*, **199**, 11-22. https://doi.org/10.1016/j.apcatb.2016.05.049

Jourshabani, M., Shariatinia, Z. and Badiei, A. (2017), "Controllable synthesis of mesoporous sulfur-doped carbon nitride materials for enhanced visible light photocatalytic degradation", *Langmuir*, **33**(28), 7062-7078. https://doi.org/10.1021/acs.langmuir.7b01767

Khan, S.B., Rahman, M.M., Marwani, H.M., Asiri, A.M. and Alamry, K.A. (2013), "An assessment of zinc oxide nanosheets as a selective adsorbent for cadmium", *Nanosc. Res. Lett.*, **8**(1), 377. https://doi.org/10.1186/1556-276X-8-377

Kim, S.P., Choi, M.Y. and Choi, H.C. (2016), "Photocatalytic activity of SnO_2 nanoparticles in methylene

blue degradation", *Mater. Res. Bull.*, **74**, 85-89. https://doi.org/10.1016/j.materresbull.2015.10.024

Kumar, S.G. and Rao, K.K. (2015), "Zinc oxide based photocatalysis: tailoring surface-bulk structure and related interfacial charge carrier dynamics for better environmental applications", *Rsc Adv.*, **5**(5), 3306-3351. https://doi.org/10.1039/C4RA13299H

Kumar, R., Rana, D., Umar, A., Sharma, P., Chauhan, S. and Chauhan, M.S. (2015), "Ag-doped ZnO nanoellipsoids: Potential scaffold for photocatalytic and sensing applications", *Talanta*, **137**, 204-213. https://doi.org/10.1016/j.talanta.2015.01.039

Kuo, W.S. and Ho, P.H. (2001), "Solar photocatalytic decolorization of methylene blue in water", *Chemosphere*, **45**(1), 77-83. https://doi.org/10.1016/S0045-6535(01)00008-X

Kuriki, R., Sekizawa, K., Ishitani, O. and Maeda, K. (2015), "Visible-light-driven CO_2 reduction with carbon nitride: enhancing the activity of ruthenium catalysts", *Angew. Chem., Int. Ed.*, **54**(8), 2406-2409. https://doi.org/10.1002/anie.201411170

Linsebigler, A.L., Lu, G. and Yates Jr, J.T. (1995), "Photocatalysis on TiO_2 surfaces: principles, mechanisms, and selected results", *Chem. Rev.*, **95**(3), 735-758. https://doi.org/10.1021/cr00035a013

Liu, G., Niu, P., Sun, C., Smith, S.C., Chen, Z., Lu, G.Q. and Cheng, H.M. (2010), "Unique electronic structure induced high photoreactivity of sulfur-doped graphitic C_3N_4", *J. Am. Chem. Soc.*, **132**(33), 11642-11648. https://doi.org/10.1021/ja103798k

Pare, B., Jonnalagadda, S., Tomar, H., Singh, P. and Bhagwat, V. (2008), "ZnO assisted photocatalytic degradation of acridine orange in aqueous solution using visible irradiation", *Desalination*, **232**, 80-90. https://doi.org/10.1016/j.desal.2008.01.007

Qamar, M.A., Shahid, S., Khan, S.A., Zaman, S. and Arwar, M.N. (2017), "Synthesis characterization, optical and antibacterial studies of Co-doped SnO_2 nanoparticles", *Digest J. Nanomater. Biostruct.*, **12**(4), 1127-1135.

Qamar, M.A., Shahid, S. and Javed, M. (2020a), "Synthesis of dynamic g-C_3N_4/Fe@ ZnO nanocomposites for environmental remediation applications", *Ceram. Int.*, **46**(14), 22171-22180. https://doi.org/10.1016/j.ceramint.2020.05.294

Qamar, M.A., Shahid, S., Javed, M., Iqbal, S., Sher, M. and Akbar, M.B. (2020b), "Highly efficient g-C3N4/Cr-ZnO nanocomposites with superior photocatalytic and antibacterial activity", *J. Photochem. Photobiol. A: Chem.*, **401**, 112776. ttps://doi.org/10.1016/j.jphotochem.2020.112776

Qamar, M.A., Javed, M., Shahid, S., Iqbal, S., Abubshait, S.A., Abubshait, H.A., Ramay. S.M., Mehmood, A and Ghaithan, H.M. (2021a), "Designing of highly active g-C_3N_4/Co@ ZnO ternary nanocomposites for the disinfection of pathogens and degradation of the organic pollutants from wastewater under visible light", *J. Environ. Chem. Eng.*, **9**(4), 105534. https://doi.org/10.1016/j.jece.2021.105534

Qamar, M.A., Shahid, S., Javed, M., Iqbal, S., Sher, M., Bahadur, A., AL-Anazy, M.M., Laref, A. and Li, D. (2021b), "Designing of highly active g-C_3N_4/Ni-ZnO photocatalyst nanocomposite for the disinfection and degradation of the organic dye under sunlight radiations", *Colloids Surf. A Physicochem. Eng. Asp.*, **614**, 126176. https://doi.org/10.1016/j.colsurfa.2021.126176

Qamar, M.A., Shahid, S., Javed, M., Sher, M., Iqbal, S., Bahadur, A. and Li, D. (2021c), "Fabricated novel g-C_3N_4/Mn doped ZnO nanocomposite as highly active photocatalyst for the disinfection of pathogens and degradation of the organic pollutants from wastewater under sunlight radiations", *Colloids Surf. A Physicochem. Eng. Asp.*, **611**, 125863. https://doi.org/10.1016/j.colsurfa.2020.125863

Ran, J., Ma, T.Y., Gao, G., Du, X.W. and Qiao, S.Z. (2015), "Porous P-doped graphitic carbon nitride nanosheets for synergistically enhanced visible-light photocatalytic H_2 production", *Energy Environ. Sci.*, **8**(12), 3708-3717. https://doi.org/10.1039/C5EE02650D

Samadi, M., Zirak, M., Naseri, A., Khorashadizade, E. and Moshfegh, A.Z. (2016), "Recent progress on doped ZnO nanostructures for visible-light photocatalysis", *Thin Solid Films*, **605**, 2-19. https://doi.org/10.1016/j.tsf.2015.12.064

Sher, M., Javed, M., Shahid, S., Hakami, O., Qamar, M.A., Iqbal, S., Al-Anazy, M.M. and Baghdadi, H.B. (2021a), "Designing of highly active g-C_3N_4/Sn doped ZnO heterostructure as a photocatalyst for the disinfection and degradation of the organic pollutants under visible light irradiation", *J. Photochem.*

Photobiol. A: *Chem*., **418**, 113393. https://doi.org/10.1016/j.jphotochem.2021.113393

Sher, M., Javed, M., Shahid, S., Iqbal, S., Qamar, M.A., Bahadur, A. and Qayyum, M.A. (2021b), "The controlled synthesis of g-C_3N_4/Cd-doped ZnO nanocomposites as potential photocatalysts for the disinfection and degradation of organic pollutants under visible light irradiation", *RSC Adv*., **11**(4), 2025-2039. https://doi.org/10.1039/d0ra08573a

Sher, M., Khan, S.A., Shahid, S., Javed, M., Qamar, M.A., Chinnathambi, A. and Almoallim, H. (2021c), "Synthesis of novel ternary hybrid g-C3N4@Ag-ZnO nanocomposite with Z-scheme enhanced solar light-driven methylene blue degradation and antibacterial activities", *J. Environ. Chem. Eng*., **9**(4), 105366. https://doi.org/10.1016/j.jece.2021.105366

Subramanian, V., Wolf, E. and Kamat, P.V. (2001), "Semiconductor-metal composite nanostructures. To what extent do metal nanoparticles improve the photocatalytic activity of TiO_2 films?", *J. Phys. Chem. B*., **105**(46), 11439-11446. https://doi.org/10.1021/jp011118k

Thi, V.H.T. and Lee, B.K. (2017), "Great improvement on tetracycline removal using ZnO rod-activated carbon fiber composite prepared with a facile microwave method", *J. Hazard. Mater*., **324**, 329-339. https://doi.org/10.1016/j.jhazmat.2016.10.066

Wang, X., Maeda, K., Chen, X., Takanabe, K., Domen, K., Hou, Y., Fu, X. and Antonietti, M. (2009), "Polymer semiconductors for artificial photosynthesis: hydrogen evolution by mesoporous graphitic carbon nitride with visible light", *J. Am. Chem. Soc*., **131**(5), 680-1681. https://doi.org/10.1021/ja809307s

Wang, Y., Li, H., Yao, J., Wang, X. and Antonietti, M. (2011), "Synthesis of boron doped polymeric carbon nitride solids and their use as metal-free catalysts for aliphatic C–H bond oxidation", *Chem. Sci*., **2**(3), 446-450. https://doi.org/10.1039/C0SC00475H

Wang, K., Li, Q., Liu, B., Cheng, B., Ho, W. and Yu, J. (2015), "Sulfur-doped g-C_3N_4 with enhanced photocatalytic CO2-reduction performance", *Appl. Catal. B*: *Environ*., **176**, 44-52. https://doi.org/10.1016/j.apcatb.2015.03.045

Zhang, J., Chen, Y. and Wang, X. (2015), "Two-dimensional covalent carbon nitride nanosheets: synthesis, functionalization, and applications", *Energy Environ. Sci*., **8**(11), 3092-3108. https://doi.org/10.1039/C5EE01895A

Zhang, W., Zhang, J., Dong, F. and Zhang, Y. (2016), "Facile synthesis of in situ phosphorus-doped gC3N4 with enhanced visible light photocatalytic property for NO purification", *Rsc Adv*., **6**(91), 88085-88089. https://doi.org/10.1039/C6RA18349B

CC